

# Synthesis and Characterization of Ruthenium Pyrochlore Oxides $\text{La}_{2-x}\text{Cd}_x\text{Ru}_2\text{O}_{7-\delta}$

W. J. Zhu, S. T. Ting, and P. H. Hor

*Department of Physics and Texas Center for Superconductivity at the University of Houston, Houston, Texas 77204-5932*

Received August 13, 1996; in revised form December 2, 1996; accepted December 5, 1996

The new metallic ruthenium pyrochlore oxides  $\text{La}_{2-x}\text{Cd}_x\text{Ru}_2\text{O}_{7-\delta}$  have been synthesized for  $x = 0.8, 1.0, 1.2, 1.4$  and  $1.6$  at temperatures between  $1050$  and  $1100^\circ\text{C}$ . Magnetization measurements for  $x = 1.0$  and  $1.6$  revealed their strong temperature-dependent paramagnetic behaviors. The bond angle  $\text{Ru-O-Ru}$  ( $137.9^\circ$ ) and bond length  $\text{Ru-O}$  ( $1.957 \text{ \AA}$ ) determined for  $\text{La}_{0.4}\text{Cd}_{1.6}\text{Ru}_2\text{O}_{7-\delta}$  are located in the region of other metallic ruthenium pyrochlore oxides. The pyrochlore phase  $\text{La}_{0.4}\text{Cd}_{1.6}\text{Ru}_2\text{O}_{7-\delta}$  after prolong annealing at  $950^\circ\text{C}$  in air converts into the nearly pure perovskite phase  $\text{La}_{0.2}\text{Cd}_{0.8}\text{RuO}_3$ . Magnetic measurement indicates that  $\text{La}_{0.2}\text{Cd}_{0.8}\text{RuO}_3$  is a weak ferromagnet with a Curie temperature of about  $37 \text{ K}$ . © 1997 Academic Press

Press

## INTRODUCTION

Ruthenium pyrochlore oxides have been extensively studied for their novel conductivity (1, 2) and catalytic activity (3, 4) which is related to their oxygen nonstoichiometry.  $\text{Bi}_2\text{Ru}_2\text{O}_7$  and  $\text{Pb}_2\text{Ru}_2\text{O}_{6.5}$  (5–7) show metallic conductivity and Pauli paramagnetism with low resistivity of  $10^{-3} \Omega\text{-cm}$  at room temperature, while rare earth ruthenates  $\text{Ln}_2\text{Ru}_2\text{O}_7$  ( $\text{Ln} = \text{Pr-Lu}$ ) and  $\text{Y}_2\text{Ru}_2\text{O}_7$  (8–10) are semiconducting with low activation energy and a spontaneous ruthenium atomic moment. Intermediate behavior was observed in  $\text{Tl}_2\text{Ru}_2\text{O}_7$  (11), which undergoes a metal-insulator (MI) transition. The solid solutions  $\text{Bi}_{2-x}\text{Ln}_x\text{Ru}_2\text{O}_7$  ( $\text{Ln} = \text{Pr-Lu, Y}$ ) (12–15) occur in the whole composition range and exhibit a MI crossover at  $40\text{--}80 \text{ K}$  for  $\text{Ln} = \text{Pr-Sm}$ . Electrical resistivity was correlated to the bend of the angle  $\text{Ru-O-Ru}$ .  $\text{Pb}_{2-x}\text{Ln}_x\text{Ru}_2\text{O}_{7-y}$  ( $\text{Ln} = \text{Nd, Gd}$ ) (16) was recently prepared and characterized by X-ray, neutron diffraction, and resistivity measurements. Ca doped  $\text{BiCaRu}_2\text{O}_{7-y}$  (17,18) is metallic and shows Curie-Weiss type paramagnetism. In the system  $\text{La}_2\text{O}_3\text{-RuO}_2$ , pyrochlore-type  $\text{La}_2\text{Ru}_2\text{O}_7$  has never been reported. Instead, the distorted metallic perovskite-type  $\text{LaRuO}_3$  (19) forms where the oxidation number of Ru is reduced to  $+3$ . Although Cd forms pyrochlore oxides with some cations of valence  $+5$

or  $+4$ , e.g.,  $\text{Cd}_2\text{Nb}_2\text{O}_7$ , such a phase has not yet been found in the system with  $\text{RuO}_2$ . Here, we report the lanthanum cadmium ruthenates  $\text{La}_{2-x}\text{Cd}_x\text{Ru}_2\text{O}_{7-y}$  with this structure type.

## EXPERIMENTAL

The compounds  $\text{La}_{2-x}\text{Cd}_x\text{Ru}_2\text{O}_{7-y}$  ( $x = 0.8, 1.0, 1.2, 1.4, 1.6$ ) were prepared from the stoichiometric quantities of  $\text{La}_2\text{O}_3$ ,  $\text{CdO}$ , and  $\text{RuO}_2$ . The thoroughly mixed powders were pelletized and pre-fired at  $950$  in air for  $24 \text{ hr}$ . Then they were reground and sintered at  $1100$  in air for  $48 \text{ hr}$  with one intermittent grinding, followed by a quench to room-temperature. X-ray diffraction was used to check phase compositions in the samples. Intensity data were collected between  $25^\circ$  and  $120^\circ$  at intervals of  $0.02^\circ$  using  $\text{CuK}\alpha$  radiation. Structure and lattice parameters were refined with a Rietveld program DBWS9411 (20). Magnetic susceptibilities were measured between  $5$  and  $300 \text{ K}$  using a SQUID magnetometer. Electrical conductivities were measured using a standard four-probe method in the temperature range from  $10$  to  $300 \text{ K}$ .

## RESULTS AND DISCUSSION

Figure 1 shows the X-ray diffraction patterns for the compositions  $\text{La}_{2-x}\text{Cd}_x\text{Ru}_2\text{O}_{7-y}$  ( $x = 0.8, 1.0, 1.2, 1.4, 1.6$ ). A single black cubic pyrochlore phase was obtained for these samples except that of  $x = 0.8$  which contains a minority perovskite phase  $(\text{La,Cd})\text{RuO}_3$ . The lattice parameters were refined to be  $10.344(6), 10.316(5), 10.273(7), 10.288(8),$  and  $10.331(5)$ , respectively. The firing temperature required to get a single-phase material is between  $1050$  and  $1100^\circ\text{C}$ . With a lower reacting temperature, samples contain unreacted  $\text{RuO}_2$ ,  $\text{CdO}$ , and the perovskite phase  $(\text{La,Cd})\text{RuO}_3$ . Higher temperature will lead to the decomposition of the pyrochlore phase due to the volatility of  $\text{RuO}_2$  and  $\text{CdO}$ . It was observed that heating the samples that were mixed with some water when making pellets rapidly converts the pyrochlore phase into  $\text{RuO}_2$  and

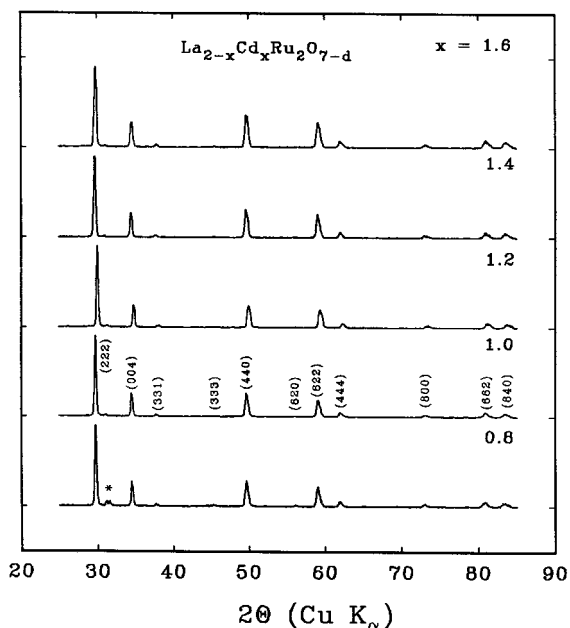


FIG. 1. X-ray diffraction patterns for  $\text{La}_{2-x}\text{Cd}_x\text{Ru}_2\text{O}_{7-y}$  ( $x = 0.8, 1.0, 1.2, 1.4, 1.6$ ) with peaks indexed on a cubic pyrochlore structure. The asterisk indicates the minority perovskite phase.

$\text{CdO}$ , especially for the  $\text{CdO}$ -rich compositions. A nearly single perovskite phase  $(\text{La}_{0.2}\text{Cd}_{0.8})\text{RuO}_3$ , as indicated in Fig. 2, was obtained when the pure pyrochlore phase  $\text{La}_{0.4}\text{Cd}_{1.6}\text{Ru}_2\text{O}_{7-y}$  was further heated at  $950^\circ\text{C}$  in air for 48 hr. Annealing at only  $250^\circ\text{C}$  in one oxygen atmosphere also causes the partial decomposition of the pyrochlore phase. Only the sample with composition  $\text{LaCdRu}_2\text{O}_{7-y}$  is nearly stable under the above conditions. The diffraction peaks for  $\text{La}_{0.4}\text{Cd}_{1.6}\text{Ru}_2\text{O}_{7-y}$  split, indicating a lower structure symmetry, probably associated with the ordering of oxygen vacancies as in the related oxygen-deficient system  $\text{Pb}_2\text{Ru}_2\text{O}_{7-y}$  determined by neutron diffraction (21).

The Structure of  $\text{La}_{0.4}\text{Cd}_{1.6}\text{Ru}_2\text{O}_{7-y}$  was refined on  $Fd\bar{3}m$ . A pseudo-Voigt peak shape function was assumed.

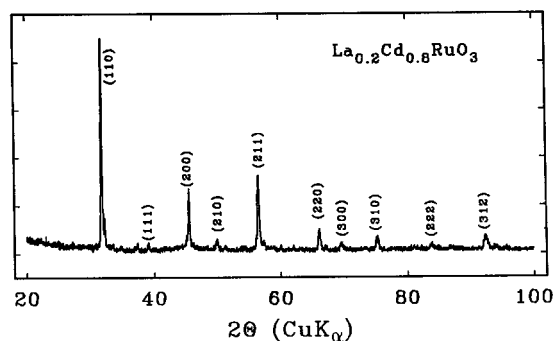


FIG. 2. X-ray diffraction pattern for perovskite phase  $\text{La}_{0.2}\text{Cd}_{0.8}\text{RuO}_3$  ( $a = 3.989(1) \text{ \AA}$ ).

TABLE 1  
Structure Parameters for  $\text{La}_{0.4}\text{Cd}_{1.6}\text{Ru}_2\text{O}_{7-y}$  (Space Group,  $Fd\bar{3}m$ ;  $a = 10.331(5) \text{ \AA}$ )

Atom	Site	$x$	$y$	$z$	Occupancy	$B(\text{Å}^2)$
La/Cd	16d	1/2	1/2	1/2	1.0	0.8(2)
Ru	16c	0	0	0	1.0	0.2(1)
O	48f	0.318(3)	1/8	1/8	1.0	1.1(3)
O'	8b	3/8	3/8	3/8	0.67(5)	1.1(3)
Ru–O(Å)	1.957(11)	La/Cd–O(Å)	2.623(22)			
La/Cd–O'(Å)	2.236(1)	Ru–O–Ru(°)	137.9(1.7)			

Note.  $R_{wp} = 8.9\%$ ,  $R_p = 7.1\%$ ,  $R_{exp} = 5.5\%$ , and  $R_1 = 7.3\%$ .

The final structure parameters are listed in Table 1 with the observed, calculated, and difference patterns shown in Fig. 3.

All these samples show metallic conductivity as indicated in Fig. 4. The resistivity is lower and shows less temperature dependence for the sample with the higher Cd content. The conducting behavior is correlated to the Ru  $4d$  bandwidth and the Ru–O overlap integrals. The bond angle Ru–O–Ru of  $\text{La}_{0.4}\text{Cd}_{1.6}\text{Ru}_2\text{O}_{7-y}$  is close to that of metallic  $\text{Bi}_2\text{Ru}_2\text{O}_7$  ( $\sim 138^\circ$ ), larger than that ( $\sim 128.5^\circ$ ) of the semiconducting phase  $\text{Y}_2\text{Ru}_2\text{O}_7$  and thus with a wider Ru  $4d$  band. The Ru–O bond length also lies in the region (about  $1.94$ – $1.97 \text{ \AA}$ ) with metallic behavior, which is shorter than that of the semiconducting phase, e.g.,  $1.986 \text{ \AA}$  for  $\text{Y}_2\text{Ru}_2\text{O}_7$ . Magnetic susceptibilities shown in Fig. 5 for  $\text{La}_{2-x}\text{Cd}_x\text{Ru}_2\text{O}_{7-y}$  ( $x = 1.6$  and  $1.0$ ) indicate a Curie–Weiss type paramagnetic behavior at high temperature above  $120 \text{ K}$ . The effective magnetic moments for Ru were determined to be  $3.1$  and  $3.2$ , respectively. They are much smaller than the value  $4.89$  for the high spin state of  $d^4$  ( $S = 2$ ), but close to  $2.83$  for its low spin state ( $S = 1$ ), suggesting that Ru that is octahedrally oxygen coordinated is at a low spin state. As compared

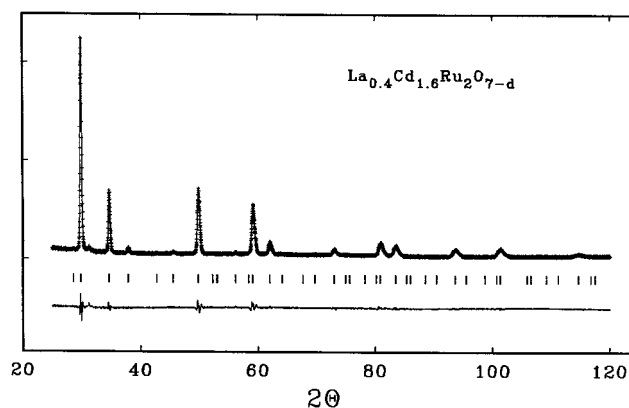


FIG. 3. Observed (–) and calculated (+) patterns with their difference shown below.

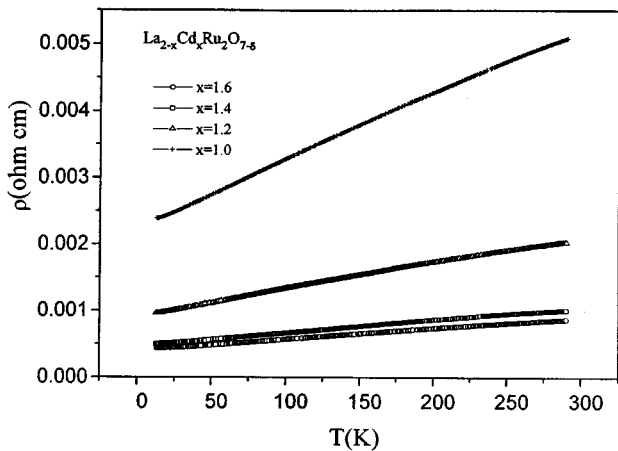


FIG. 4. Temperature dependence of resistivity for  $\text{La}_{2-x}\text{Cd}_x\text{Ru}_2\text{O}_{7-y}$  ( $x = 0.8, 1.0, 1.2, 1.4, 1.6$ ).

with the related stoichiometric ruthenium pyrochlore series,  $\text{Ln}_2\text{Ru}_2\text{O}_7$  ( $\text{Ln} = \text{rare earth and Y}$ ) (9) which gives almost the same effective moment as the low spin state of  $\text{Ru}^{4+}$ , the slightly higher values for  $\text{La}_{2-x}\text{Cd}_x\text{Ru}_2\text{O}_{7-y}$  can be ascribed to the mixed valence of Ru with the estimated Ru oxidation states  $+4.26$  and  $+4.35$  and thus the oxygen content derived  $y = 0.54$  and  $0.15$  for  $\text{La}_{0.4}\text{Cd}_{1.6}\text{Ru}_2\text{O}_{7-y}$  and  $\text{LaCdRu}_2\text{O}_{7-y}$ , respectively. The negative paramagnetic Curie temperature for both compounds indicates an antiferromagnetic coupling between the Ru cations. The large temperature dependence of inverse magnetic susceptibilities at low temperature below 50 K probably is due to the enhancement of exchange interaction between electrons of the conduction band, as in the case of  $\text{BiCaRu}_2\text{O}_{7-y}$ . Figure 6 shows the field-cooled magnetic susceptibility data

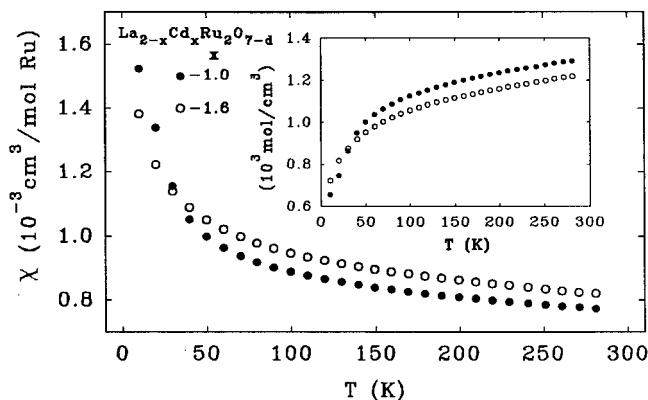


FIG. 5. Magnetic susceptibilities for  $\text{La}_{2-x}\text{Cd}_x\text{Ru}_2\text{O}_{7-y}$  ( $x = 1.0$  and  $1.6$ ) with strong temperature dependence and large magnetic moments for Ru.

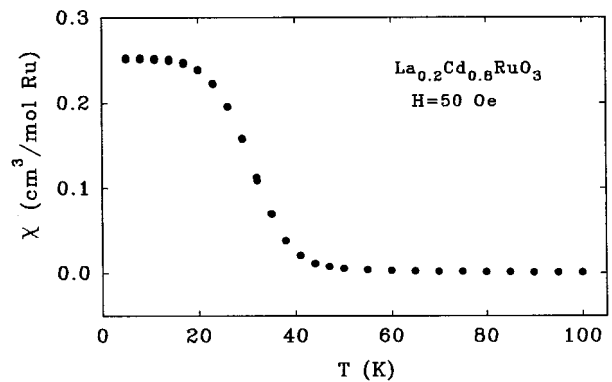


FIG. 6. Magnetic susceptibility measured at FC mode for perovskite phase  $\text{La}_{0.2}\text{Cd}_{0.8}\text{RuO}_3$  ( $a = 3.985(2)\text{\AA}$ ), indicating the ferromagnetic transition around 37 K.

for the cubic perovskite phase  $(\text{La}_{0.2}\text{Cd}_{0.8})\text{RuO}_3$ ; a spontaneous magnetization develops around 37 K, indicating a weak ferromagnetic transition for this compound. Field and zero-field susceptibilities are consistent.  $\text{SrRuO}_3$  was known to be a ferromagnet with  $T_C = 160$  K, while  $\text{CaRuO}_3$  is paramagnetic. The solid solutions  $\text{Sr}_{1-x}\text{Pb}_x\text{RuO}_3$  and  $\text{Sr}_{1-x}\text{Ca}_x\text{RuO}_3$  lie in between.  $(\text{La}_{0.2}\text{Cd}_{0.8})\text{RuO}_3$ , which is also associated with mixed valences of Ru, is expected to be similar to  $(\text{La}_{0.2}\text{Sr}_{0.8})\text{RuO}_3$ , where the end member  $\text{LaRuO}_3$  that has the  $\text{GdFeO}_3$ -type structure is metallic with paramagnetic behavior.

In summary, the lanthanum pyrochlore ruthenates  $\text{La}_{2-x}\text{Cd}_x\text{Ru}_2\text{O}_{7-y}$  ( $x = 0.8, 1.0, 1.2, 1.4, 1.6$ ) have been synthesized by codoping with cadmium. They are all metallic but show large paramagnetic susceptibilities. More detailed structure concerning oxygen occupancies, positions, and ordering will be further determined by neutron diffraction. Studies of conductivities and magnetization of the new ferromagnetic perovskite-type solid solution  $(\text{La}, \text{Cd})\text{RuO}_3$  and possible substitution of Cd at the Ru site are underway.

## ACKNOWLEDGMENTS

This work was partially supported by NSF Low Temperature Physics Program Grant DMR 9122043, ARPA Grant MDA 972-90-J-1001, and the Texas Center for Superconductivity at the University of Houston.

## REFERENCES

1. G. E. Pike and C. H. Seager, *J. Appl. Phys.* **48**, 5152(1977).
2. P. F. Carcia, A. Ferreti, and A. Suna, *J. Appl. Phys.* **53**, 5282 (1982).
3. H. S. Horowitz, J. M. Longo, and H. H. Horowitz, *J. Electrochem. Soc.* **130**, 1851 (1983).
4. R. G. Egdell, J. B. Goodenough, A. Hamnett, and C.C. Naish, *J. Chem. Soc. Faraday Trans. 1* **79**, 893(1983).
5. R. J. Bouchard and J. L. Gillson, *Mater. Res. Bull.* **6**, 669 (1971).
6. J. M. Longo, P. M. Raccach, and J. B. Goodenough, *Mater. Res. Bull.* **4**, 191 (1969).

7. R. A. Beyerlein, H. S. Horowitz, and J. M. Longo, *J. Solid State Chem.* **72**, 2 (1988).
8. E. F. Bertaut, F. Forrat, and M. C. Montmory, *C. R. Acad. Sci.* **249**, 829 (1959).
9. R. Aleonard, E. F. Bertaut, and M. C. Montmory, *J. Appl. Phys.* **33**, 1205 (1962).
10. A. W. Sleight and R. J. Bouchard, *Solid State Chem. NBS Special Publ.* **364**, 227 (1972).
11. A. W. Sleight and J. L. Gillson, *Mater. Res. Bull.* **6**, 78 (1971).
12. A. Ehmann and S. Kemmler-Sack, *Mater. Res. Bull.* **20**, 437 (1985).
13. J. B. Goodenough, A. Hamnett, and D. Telles, in "Localization and Metal Insulator Transition" (H. Fritzsche and D. Adler, Eds.), Plenum, New York, 1985.
14. R. Kanno, Y. Takeda, T. Yamamoto, Y. Kawamoto, and O. Yamamoto, *J. Solid State Chem.* **102**, 106 (1993).
15. T. Yamamoto, R. Kanno, Y. Takeda, O. Yamamoto, Y. Kawamoto, and M. Takano, *J. Solid State Chem.* **109**, 372 (1994).
16. H. Kobayashi, R. Kanno, Y. Kawamoto, T. Kamiyama, F. Izumi, and A.W. Sleight, *J. Solid State Chem.* **114**, 15 (1995).
17. M. Schuler and S. Kemmler-sack, *J. Less-Comm. Met.* **102**, 105 (1984);
18. B.J. Kennedy, *J. Solid State Chem.* **119**, 254 (1995).
19. R. J. Bouchard and J. F. Weiher, *J. Solid State Chem.* **4**, 80 (1972).
20. R. A. Young, A. Sakthivel, T. S. Moss, and C. O. Paiva-Santos, *J. Appl. Crystallogr.* **28**, 366 (1995).
21. R. A. Beyerlein, H. S. Horowitz, J. M. Longo and M. E. Leonowicz, *J. Solid State Chem.* **51**, 253 (1995).